CFD study of gas-liquid hydrodynamics in a bubble column

Mohd Shahimie Selamat, Jolius Gimbun[†]

ABSTRACT

This paper presents a computational fluid dynamics (CFD) of the gas-liquid flow in a bubble column. Multiphase simulations were performed using an Eulerian-Eulerian two-fluid model besides considering the drag coefficient model suitable for spherical and distorted bubbles. The interfacial force modelling also considered the effect of the void fractions on the drag coefficient. The CFD predictions were compared to the experimental measurement adopted from literature. The CFD predicts the turbulent kinetic energy, gas hold-up and the liquid axial velocity fairly well, although the results seem to suggest that further improvement to both the interfacial force model and two-fluid modeling approaches is necessary. It is clear from the modeling exercise performed in this work that CFD is a promising method for modeling the performance of bubble column. Furthermore, the CFD method is certainly less expensive than the experimental characterization studies.

Key words: Bubble column; Gas-liquid; Eulerian-eulerian; Interphase drag modeling

INTRODUCTION

Bubble column is often used in variety industrial applications, especially petrochemical and biochemical processes as reactors or gas-liquid contactors. Bubble columns had an advantage of being mechanically simple without present of any internal structure or moving part, thus leading to easier maintenance. They also have high mass transfer rates between the gas and liquid phases, good heat transfer characteristics and large liquid hold-up, which are favourable to slow liquid phase reactions (Shah *et al*., 1982). Operation of bubble columns is often determined by several global parameters such as pressure drop, aeration height and gas superficial velocity. However, the variables that affect the performance of bubble column are the gas hold-up distribution, gas-liquid mass and heat transfer coefficients, the extent of mixing, bubble rise velocities and bubble size distributions. It is possible to measure these variables experimentally using, for example, a combination of several instruments such as the laser doppler anemometry, dissolved oxygen probe, X-ray tomography and digital imaging. However, experimental measurements require investing in costly instruments and building a prototype. Alternatively, these parameters can also be obtained from CFD simulations, which offer a cheaper but much faster solution.

CFD has proven itself as a valuable tool for gaining insight in flow phenomena in general and complex multiphase flows arising in process equipment in particular (Dijkhuizen *et al*., 2010). Computational fluid dynamics (CFD) is one of the branches of fluid mechanics that uses numerical methods and algorithms to solve and analyze problems that involve fluid flows. CFD simulation is applicable to a variety of gas-liquid dispersion problems including bubble column (Ekambara *et al*., 2005; Kulkarni *et al*., 2007; Gimbun, 2009), which offer a cheaper but with a faster solution compared with measuring using experimental instrumentation. Most of the time the Eulerian-Eulerian two-fluid model was employed to solve the two phase problem and the dispersed k-ε model was used for turbulence modeling.

Many studies related with bubble column modeling and the simulations have been carried out for the predictions of flow pattern in bubble column reactors using 1D, 2D and 3D mathematical models in the past. All these models showed good agreement with the experimental measurement for axial liquid velocity and the fractional gas hold-up (Ekambara *et al*., 2005). Kulkarni *et al*. (2007), reported the profiles of axial mean liquid velocity at various heights, which shows the development of flow pattern in a bubble column and the same can also be seen from the fractional gas hold-up profiles. The CFD predictions were seen to have an excellent match with the experimental measurements (Ekambara *et al*., 2005; Kulkarni *et al*., 2007; Gimbun, 2009; Li *et al*., 2009; Dhotre and Joshi, 2007). CFD simulations were also employed to evaluate effects of the configuration of gas distributors to the gas–liquid flow and mixing in a bubble column (Li *et al*., 2009; Dhotre and Joshi, 2007), modelling slurry reactor for Fischer Tropsch synthesis (Maretto and Krishna, 1999; Troshko and Zdravistch, 2009) and dynamic flow behavior (Zhang *et al*., 2006; Pfleger and Becker, 2001). Other related studies reported that the simulation (CFD) results indicate that the Eulerian-Eulerian formulation is a promising approach to predict the hydrodynamics of bubble column. CFD provides good engineering descriptions, and can be used reliably for predicting the flow and hold-up patterns in bubble columns (Mousavi *et al*., 2008; Dhotre *et al*., 2005; Selma *et al*., 2010). However, less attention was paid to the effect of the drag coefficient to the prediction of turbulent kinetic energy. Therefore, the aim of this work is to develop a three dimensional CFD model to study the influence of the interfacial drag coefficient to the turbulent kinetic energy, gas hold-up profile and the liquid axial velocity in bubble column.

COMPUTATIONAL APPROACH

The Eulerian-Eulerian approach is employed for gas-liquid bubble column simulation in this work, whereby the continuous and disperse phases are considered as interpenetrating media, identified by their local volume fractions.

The volume fractions sum to unity and are governed by the following continuity equations:

$$\frac{\partial}{\partial t}(\alpha_l \rho_l) + \nabla \cdot (\alpha_l \rho_l \vec{u}_l) = 0 \tag{1}$$

where α_l is the liquid volume fraction, ρ_l is the density, and $\vec{u}_l$ is the velocity of the liquid phase. The mass transferred between phases is negligibly small and hence is not included in the right hand-side of eq.(1). A similar equation is solved for the volume fraction of the gas phase by replacing the subscript *l* with *g* for gas. The momentum balance for the liquid phase is:

$$\frac{\partial}{\partial t}(\alpha_l \rho_l \vec{u}_l) + \nabla \cdot (\alpha_l \rho_l \vec{u}_l \vec{u}_l) = -\alpha_l \nabla P + \nabla \cdot \bar{\bar{\tau}}_l + \vec{F}_{\mathrm{lg}} + \alpha_l \rho_l \vec{g} + \vec{F}_{lift,l} + \vec{F}_{vm,l} \tag{2}$$

where $\bar{\bar{\tau}}_l$ is the liquid phase stress-strain tensor, $\vec{F}_{lift,l}$ is a lift force, $\vec{g}$ is the acceleration due to gravity and $\vec{F}_{vm,l}$ is the virtual mass force. A similar equation is solved for the gas phase. $\vec{F}_{\mathrm{lg}}$ is the interaction force between phases, due to drag. Hence, $\vec{F}_{\mathrm{lg}}$ is represented by a simple interaction term for the drag force, given by:

$$\vec{F}_{\mathrm{lg}} = -\frac{3\alpha_g \alpha_l C_D \left|\vec{u}_g - \vec{u}_l\right| \left(\vec{u}_g - \vec{u}_l\right)}{4 d_b} \tag{3}$$

where C_D is a drag coefficient and d_b is the Sauter mean bubble diameter.

The drag model employed has a significant effect on the flow field of the aerated flow, as it is related directly to the bubble terminal rise velocity (Gimbun *et al*., 2009). Bubbles have a tendency to form a non-spherical shape, especially those with a diameter less than 3 mm. Therefore, the drag model of Tomiyama *et al*. (1995) was selected in this work, as it takes into account the drag of distorted bubbles:

$$C_{Dm} = \max\left[\min\left\{\frac{16}{\mathrm{Re}_b}\left(1 + 0.15\,\mathrm{Re}_b^{0.687}\right), \frac{48}{\mathrm{Re}_b}\right\}, \frac{8}{3}\frac{E_O}{E_O + 4}\right] \tag{4}$$

where the Re and E_O are the bubble Reynolds number and Eotvos number, respectively. The drag for the ellipsoidal bubble regime is dependent on the bubble shape through the Eotvos number, which represents the ratio of gravitational to

surface tension forces; for the spherical cap regime the drag coefficient is approximately 8/3. The effect of the local bubble volume fraction on the drag coefficient is estimated using Behzadi et al.'s (2004) correlation as follows:

$$C_{D,dense} = C_D\left(e^{3.64\alpha} + \alpha^{0.864}\right) \tag{5}$$

where the C_D is the drag coefficient for isolated bubble estimated using Eq. (4), whereas $C_{D,dense}$ is for the dense dispersion of bubbles. The drag model described above is not available as a standard option in FLUENT and hence it has been implemented via a user-defined subroutine (UDF).

Lift forces act on a bubble due to the velocity gradients in the liquid phase and are said to be more significant for larger bubbles. The lift force acting on a gas phase in a liquid phase can be estimated from:

$$\vec{F}_{lift,g} = -C_L\rho_l\alpha_g\left(\vec{u}_l - \vec{u}_g\right)\times\left(\nabla\times\vec{u}_l\right) \tag{6}$$

where C_L is a lift coefficient has a value 0.5. A similar lift force is added to the right-hand side of the momentum equation for both phases ($\vec{F}_{lift,g} = -\vec{F}_{lift,l}$).

The virtual mass effect occurs when a gas phase accelerates relative to the liquid phase. The fluid surrounding the bubble is accelerating as a consequence of the bubble acceleration. This gives a rise to a force called a virtual mass which accounts for the losses of momentum of the accelerating bubble. The virtual mass force acting on bubbles is given by:

$$\vec{F}_{vm,g} = C_m\rho_l\alpha_g\left(\frac{d_l\vec{u}_l}{dt} - \frac{d_g\vec{u}_g}{dt}\right) \tag{7}$$

where C_m is the added mass coefficient has a value 0.5 for sphere. Similar with the lift force the virtual mass force is added to the right-hand side of the momentum equation for both phases ($\vec{F}_{vm,l} = -\vec{F}_{vm,g}$).

Turbulence modeling was realized using the dispersed k-ε model which is suitable when the secondary phase is dilute and the primary phase is clearly continuous; the dispersed k-ε turbulence model is used and solves the standard k-ε equations for the primary phase. The liquid turbulent viscosity, $\mu_{t,l}$, is written as:

$$\mu_{t,l} = \rho_l C_\mu \frac{k_l^2}{\varepsilon_l} \tag{8}$$

The transport equations for k and ε in the dispersed k-ε model are given by:

$$\frac{\partial}{\partial t}(\rho_l \alpha_l k_l) + \nabla \cdot (\rho_l \alpha_l \vec{u}_l k_l) = \nabla \cdot \left(\alpha_l \frac{\mu_{t,l}}{\sigma_k} \nabla k_l \right) + \alpha_l G_{k,l} - \alpha_l \rho_l \varepsilon_l + \alpha_l \rho_l \Pi_{k,l} \tag{9}$$

$$\frac{\partial}{\partial t}(\rho_l \alpha_l \varepsilon_l) + \nabla \cdot (\rho_l \alpha_l \vec{u}_l \varepsilon_l) = \nabla \cdot \left(\alpha_l \frac{\mu_{t,l}}{\sigma_\varepsilon} \nabla \varepsilon_l \right) + \alpha_l \frac{\varepsilon_l}{k_l} \left(C_{1,\varepsilon} G_{k,l} - C_{2,\varepsilon} \rho_l \varepsilon_l \right) + \alpha_l \rho_l \Pi_{\varepsilon,l} \tag{10}$$

$G_{k,l}$ is the rate of production of turbulent kinetic energy and it has a similar form to the one applied for single phase flow. The terms $\Pi_{k,l}$ and $\Pi_{\varepsilon,l}$ represent the influence of the dispersed phase on the continuous phase and are modelled following Elgobashi and Abou-Arab (1983). The turbulent quantities for the dispersed phase like turbulent kinetic energy and turbulent viscosity of the gas are modelled following Mudde and Simonin (1999), using the primary phase turbulent quantities (Fluent, 2006). The model constants are similar to those of mixture k-ε models.

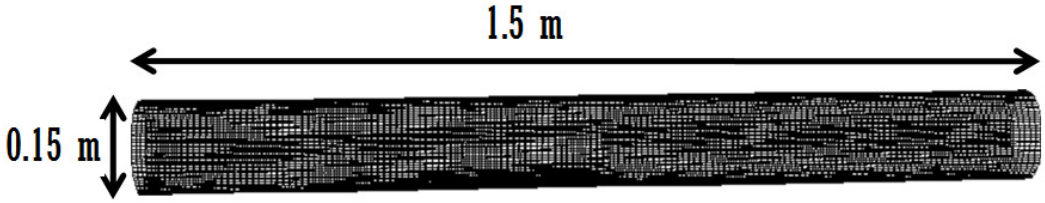

Fig. 1: Bubble column dimension and the computational grid

A cylindrical bubble column was considered with an internal diameter of 0.15 m, filled with tap water to a height of 0.9 m. The gas superficial velocity was 0.02 m/s, introduced through multipoint sparger (0.25% free area, d_0 = 1.96 mm). The bubble size is assumed constant at d_b = 0.0047 m estimated using the correlation proposed by Wilkinson (1991). The geometry of the bubble column studied here was similar to the one that has been studied experimentally and simulated numerically by Kulkarni *et al*. (2007).

The Eulerian two-fluid model was employed throughout this study with constant bubble sizes of 4.7 mm. The transient solvers with first order implicit time advancement. The interphase drag coefficient was estimated using the Tomiyama *et al*. (1995) drag model and virtual mass was also included. The top

liquid surface was allowed to expand freely as a result of aeration by applying a free surface boundary.

The grid used in this study was generated by pre-processor software, GAMBIT 2.4, contains approximately 177786 cells. The grid was made of high quality pure hexahedral mesh to minimize the turbulent diffusion during the simulation. The excess volume in the headspace is necessary because at the initial stages of the simulation, there are some major fluctuations of the liquid surface; without this excess volume, some part of the liquid would flow out from the domain and hence may cause error to the final result. In light with this issue, the final grid height was extended up to 1.5 m, to provide a more satisfactory simulation. In turbulent bubbly flow, as the flow becomes unstable and the bubbles cluster into swarms, hence regions of relatively high and low gas fractions can be distinguished. The motion of swarms through the column is highly irregular and the swarms only exist for a short period of time (Groen, 2004). The swarms dominate the hydrodynamic behavior of a bubble column by increasing the degree of (back) mixing or dispersion of the liquid phase leading to larger-scale circulation patterns. The long-time-averaged liquid flow field shows a large overall liquid circulation pattern with the liquid phase flows upward in the centre of the column and downward in the wall region (Groen, 2001).

The grid employed in this work is finer that those used by Gimbun (2009) to better predict turbulence related quantities (k and ε), and hence evaluating their effect to the CFD prediction of two-phase flow. Previous work by Gimbun (2009), showed that coarser computational grid with ranged from 6000 to 43000 cells are capable of resolving the two-phase flow in bubble column well with little difference shown on the result obtained from CFD simulation running at different grid density. Thus the grid dependent study is not necessary for this work since the grid employed in this work is more than four times (177786 cells) than the ones previously studied by Gimbun (2009) and the result should be grid independent. All result presented in this paper are taken at H/D = 1.4, H/D = 2.6 and H/D = 3.9, and are time-averages of up to 1000 time step after a steady aerated liquid level is attained similar to those measured experimentally by Kulkarni *et al*. (2007).

Water with a volume fraction of 1.0 is patched to $0 \leq z \leq 0.9$ (initial liquid height) before running the simulation, whereas water volume fraction of 0 is patched to the headspace ($0.9 \leq z \leq 1.5$). Air enters the bottom of the column using a velocity inlet boundary (gas inlet velocity equal to superficial gas velocity) as soon as the simulation started (time = 0 s).

RESULT AND DISCUSSION

The CFD predictions for the axial liquid velocity, gas hold-up and turbulent kinetic energy was compared to the experimental measurement by Kulkarni *et al*. (2007). Data from CFD simulation were taken as a statistical average from up to 1000 time step after pseudo steady-state flow was achieved (i.e. when the aerated liquid level no longer changing), which is comparable to the data collection in experimental measurement.

The mean axial liquid velocity (Fig. 2) shows that the liquid had a central upward movement and downward near the wall. The solid blue line corresponds to the CFD predictions using the drag model by Tomiyama *et al*. (1995) and the dotted green line is a result obtained from Schiller and Naumann (1935) model. The centre line liquid velocity was seen to vary with the axial level. The liquid velocity is affected by the bubble size; bigger bubbles might increase the axial velocity due to their larger bubble rise velocity but at the same time the downward recirculation also becomes larger. Other than that, the momentum from the liquid recirculation is bigger than the one induced by bubble rise velocity, and therefore, a bigger bubble size leads to a lower axial liquid velocity.

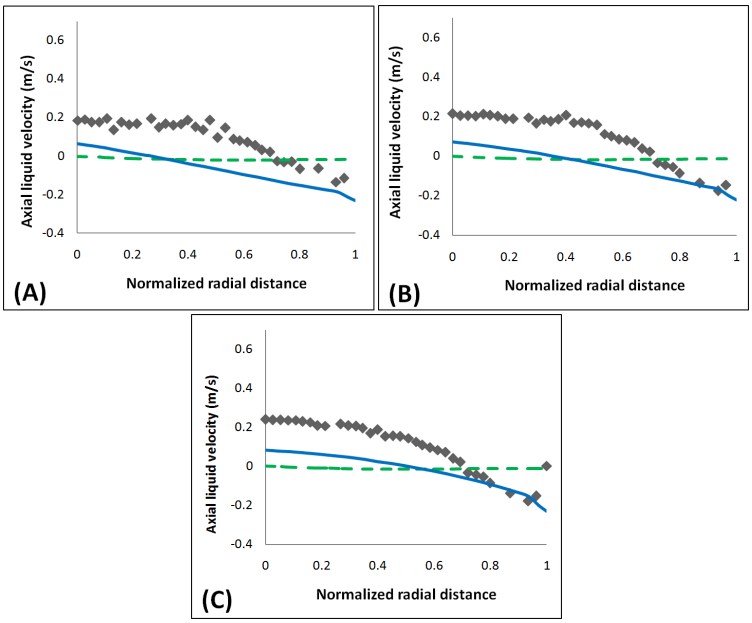

Fig. 2: Comparison between simulated and experimental profile of axial liquid velocity: (a) H/D = 1.4; (b) H/D = 2.6; (c) H/D = 3.9. Data points from Kulkarni *et al*. (2007).

As shown in Fig. 2, Tomiyama *et al.*'s (1995) model seems to have better prediction compared with the Schiller and Naumann (1935). The standard option model gives straight linear result and cannot give closer prediction in correspondent to experimental data. The modified model gives more realistic prediction which is of similar trend to the experimental data. This is attributed by the use of non-spherical drag model by Tomiyama *et al.* (1995) instead of only spherical model in Schiller and Naumann (1935).

In a bubble column reactor, the hold-up profile shows little variation throughout the column from the sparger to the disengagement zone as it shown in Fig. 3, although the axial liquid velocity may vary especially in the column centre region. Away from the sparger, more bubbles were brought towards the centre and less towards the wall Kulkarni *et al.* (2007), and consequently higher axial velocity towards the column centreline was observed.

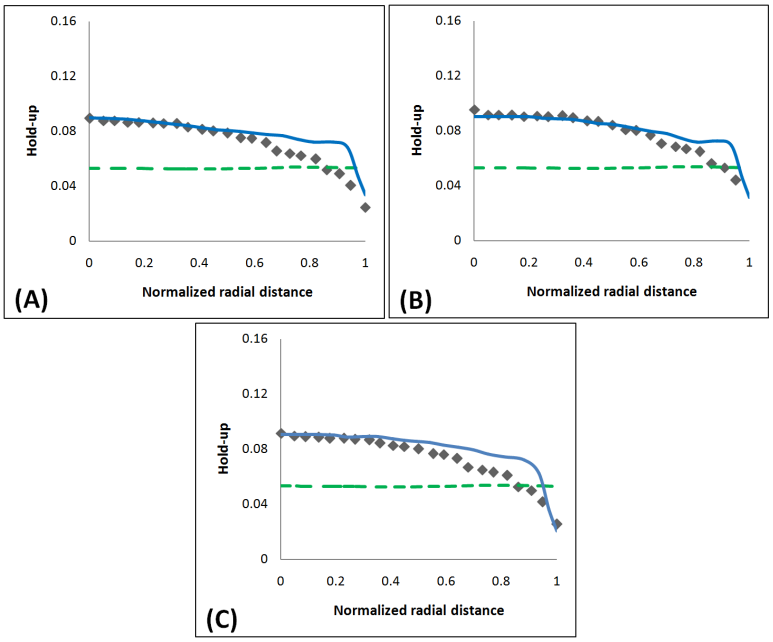

Fig. 3: Comparison between simulated and experimental profile of fractional gas hold-up: (a) H/D = 1.4; (b) H/D = 2.6; (c) H/D = 3.9. Data points from Kulkarni *et al.* (2007).

The CFD simulation also gives excellent prediction on the gas hold-up profile (Fig. 2) which is in good agreement with the experimental measurement by Kulkarni *et al.* (2007). For the same reason as in section 4.2, Tomiyama *et al.* (1995) model also gives better prediction than the Schiller and Naumann (1935)

model. The simulation results shows that the default model in FLUENT 6.3 cannot give a realistic prediction of gas hold-up profile in bubble column. This is due to the fact that bubbles larger than 3 mm is no longer spherical and hence the default model which assume spherical bubbles is no longer applicable.

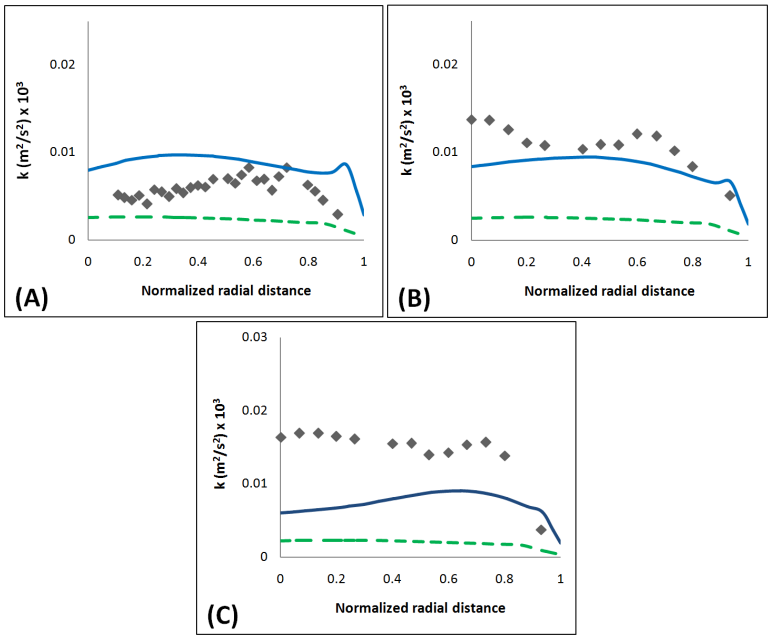

Fig. 4: Comparison between simulated and experimental profile of turbulent kinetic energy: (a) H/D = 1.4; (b) H/D = 2.6; (c) H/D = 3.9. Data points from Kulkarni *et al*. (2007).

Turbulent kinetic energy was found to have almost constant value in the central region and decreased towards the wall, and increased away from the sparger as shown in Fig. 4. The energy associated with liquid is much lesser at the bottom than at the top and part of the gas phase energy is used in pumping liquid from bottom to top. On the other word, bubble moves at different velocities depending upon the surrounding flow field. The liquid velocity is different at different positions and as a result the bubbles rise at a velocity higher in the central region and lower in the near wall region. Thus, the energy supplied by a bubble to liquid is more in the centre and less in the near wall region (Kulkarni *et al.*, 2007). The liquid velocity also increases in the upper region of the bubble column as shown in Fig. 2, which explain why the turbulent kinetics energy tends to be higher in the upper region of the column in Fig. 4.

There is some discrepancy on the CFD prediction, especially at H/D = 1.4, which may be attributed by the assumption of isotropic eddy viscosity in the *k-ε* turbulence model. The gas-liquid flow in bubble column may become anisotropic due to the bubble movement upwards and the liquid moves in the opposite direction resulting in a circulation flow. The drag model by Tomiyama *et al*. (1995) was proven to be a better drag model for the flow field at the aerated flow compared to the Schiller and Naumann (1935) drag model. This is due to a better prediction of gas hold-up and the mean velocities profile by the Tomiyama *et al*.'s (1995) model which in turn affecting the prediction accuracy for the turbulent kinetic energy.

Some of the predicted value in Fig. 1 to 3 varies from the experimental data, because as the bubble rises and the liquid moves upward and downward the bubble size may change due to the turbulence flow and velocity influence. Although, this effect may not be very significant for gas-liquid flow in a bubble column due to their tendency to become equilibrium with turbulence intensity. Nevertheless there is still a possibility of non-uniform bubble size especially near the wall where the turbulence intensity is much lesser. Furthermore, effect of the non-uniform bubble size was not considered in this work, which may have affected the accuracy of CFD prediction.

CONCLUSION

The CFD predictions of the gas hold-up show an excellent agreement between the predicted and the experimental profiles of hold-up were observed. The turbulent kinetic energy and axial liquid velocity was also predicted fairly well, although the prediction deviate from the experimental value at the upper region of the bubble column, which may be attributed by the assumption of isotropic eddy viscosity in the *k-ε* turbulence model. There are some discrepancy in the CFD predictions due to bubble breakage and coalescence as they rises inside the column. Furthermore, effect of the non-uniform bubble size was not considered in this work, which may have affected the accuracy of CFD prediction.

ACKNOWLEDGMENT

We acknowledge the research funding from UMP through the grant no. RDU0903110. Mohd Shahimie Selamat acknowledge moral support from Aiman Hakim, Siti Ferdaus, Siti Masita, Azri and Wan Mohamed Irman.

REFERENCES

Behzadi A, Issa RI and Rusche H, 2004, Modelling of dispersed bubble and droplet flow at high phase fractions, *Chem. Eng. Sci*., **59**: 759–770.

Dhotre MT and Joshi JB, 2007, Design of a gas distributor: three-dimensional CFD simulation of a coupled system consisting of a gas chamber and a bubble column, *Chem. Eng. J*., **125**: 149–163.

Dhotre MT, Vitankar VS, Joshi JB, 2005, CFD simulation of steady state heat transfer in bubble columns, *Chem. Eng. J.*, **108**: 117–125.

Dijkhuizen W, van Sint Annaland M, and Kuipers JAM, 2010, Numerical and experimental investigation of the lift force on single bubbles. *Chem. Eng. Sci.*, **65**: 1274–1287.

Ekambara K, Dhotre MT and Joshi JB, 2005, CFD simulations of bubble column reactors: 1D, 2D and 3D approach, *Chem. Eng. Sci.*, **60**: 6733–6746.

Elgobashi SE and Abou-Arab TW, 1983, A Two-Equation Turbulence Model for Two-Phase Flows, *Physic of Fluids*, **26**: 931-938.

FLUENT 6.3, User Guide, 2006.

Gimbun J, 2009, Assessment of turbulence models for modelling of bubble column, *Journal IEM*, **70**: 57-64.

Gimbun J, Rielly CD and Nagy ZK, 2009, Modelling of mass transfer in gas–liquid stirred tanks agitated by Rushton turbine and CD-6 impeller: A scale-up study, *Chem Eng. Res. Des.*, **87**: 437–451.

Groen JS, 2004, *Scales and structures in bubbly flows*, PhD Thesis, Delft University of Technology, The Netherlands.

Kulkarni AA, Ekambara K and Joshi JB, 2007, On the development of flow pattern in a bubble column reactor: Experiments and CFD, *Chem. Eng. Sci.*, **62**: 1049-1072.

Li G, Yang X and Dai G, 2009, CFD simulation of effects of the configuration of gas distributors on gas–liquid flow and mixing in a bubble column, *Chem. Eng. Sci.*, **64**: 5104-5116.

Maretto C and Krishna R, 1999, Modelling of a bubble column slurry reactor for Fischer –Tropsch synthesis, *Catalysis Today*, **52**: 279-289.

Mousavi SM, Jafari A, Yaghmaei S, Vossoughi M, Turunen I, 2008, Experiments and CFD simulation of ferrous biooxidation in a bubble column bioreactor, *Comput. Chem. Eng.*, **32**: 1681–1688.

Mudde R and Simonin O, 1999, Two and three-dimensional simulations of a bubble plume using a two-fluid model, *Chem. Eng. Sci.*, **54**: 5061–5069.

Pfleger, D. and Becker, S., 2001, Modelling and simulation of the dynamic flow behavior in a bubble column, *Chem. Eng. Sci.*, **56**: 1737-1747.

Selma B, Bannari R and Proulx P, 2010, Simulation of bubbly flows: Comparison between direct quadrature method of moments (DQMOM) and method of classes (CM), *Chem. Eng. Sci.*, **65**: 1925–1941.

Schiller L and Naumann Z, 1935, A drag coefficient correlation, *Zeitschrift Verein Deutscher Ingenieure*, **77**: 318-320.

Shah YT, Kelkar BG, Godbole SP and Deckwer WD, 1982, Design parameter estimations for bubble column reactors, *AIChE Journal*, **28**: 353-379.

Troshko AA and Zdravistch F, 2009, CFD modeling of slurry bubble column reactors for Fisher–Tropsch synthesis, *Chem. Eng. Sci*., 64: 892-903.

Tomiyama A, Kataoka I and Sakaguchi T, 1995, Drag coefficients of bubbles: 1st report, drag coefficients of a single bubble in a stagnant liquid, *Trans. JSME,* **61**: 2357–2364.

Wilkinson PM, 1991, *Physical Aspects and Scale-up of High Pressure Bubble Columns*, D.Sc. Thesis, University of Groningen, The Netherlands, 1991.

Zhang D, Deen NG and Kuipers JAM, 2006, Numerical simulation of the dynamic flow behavior in a bubble column: A study of closures for turbulence and interface forces, *Chem. Eng. Sci*., **61**: 7593–7608.

Mohd Shahimie Selamat, Jolius Gimbun†
Faculty of Chemical and Natural Resources Engineering, Universiti Malaysia Pahang, 26300 Gambang, Pahang Darul Makmur, Malaysia.
Correspondence: jolius@ump.edu.my